Compact wavelength detection system incorporating a guided-mode resonance filter

Nikhil Ganesh, Alan Xiang, Neill B. Beltran, Dennis W. Dobbs, and Brian T. Cunningham[a)]
Nano Sensors Group, Micro and Nanotechnology Laboratory, University of Illinois at Urbana-Champaign, 208 North Wright Street, Urbana, Illinois 61801

(Received 24 November 2006; accepted 18 January 2007; published online 21 February 2007)

The authors demonstrate a compact system for the detection of the peak wavelength value emitted by a light source. The system is composed of only two components, a graded-wavelength guided-mode resonance filter placed before a charge-coupled device sensor array. The filter provides a spatially resolved transmission minimum, the position of which is controlled by the wavelength of the incoming light. The sensor array collects the spatially resolved transmitted intensity and the wavelength is determined by recording the position of the transmission minimum along its length. Using this technique, wavelength changes as small as 0.011 nm can be detected. © *2007 American Institute of Physics*. [DOI: 10.1063/1.2591342]

For a wide range of spectroscopic applications, it is required to provide the spatially resolved spectrum of an incident optical beam. Typically, diffraction gratings operating in the Raman-Nath regime and prisms can provide such resolution through multiorder diffracted waves and dispersion effects, respectively. However, the need to develop cost-effective, portable solutions that can provide improved resolution and efficiency has driven the search for alternative solutions. In this study, we develop a highly cost-effective and compact system for the spectral resolution of an incident optical beam by the use of the guided-mode resonance effect. Such a system is shown to have high resolution and is comprised of only two working elements, namely, a graded-wavelength guided-mode resonance filter [hereafter refered to as a graded-wavelength filter (GWF)] and a line camera based on linear charge-coupled device (CCD) sensor array. By appropriately adjusting the physical parameters that govern the GWF function, operation can be achieved at a wide range of optical wavelengths and at a high resolution.

It was shown by Wang and Magnusson[1] and Wang *et al.*[2] that compact structures incorporating a subwavelength grating coupled to a waveguide can result in a resonance phenomenon, wherein guided modes of the waveguide are excited through higher evanescent diffracted orders of the grating. However, unlike guided modes in a strict sense, it was shown that these modes are leaky and therefore guided for a finite amount of time as they are reradiated both in the forward (transmitted) and backward (specular) directions from the structure. These reradiated waves destructively and constructively interfere with the zeroth forward and backward diffracted orders, respectively, resulting in a strong reflection at a resonant wavelength. Since the structures [referred to as guided-mode resonance filters (GMRFs)] are designed to operate in the zeroth order regime, the reflectivity for the resonant wavelength is 100%, practically limited only by fabrication defects, material losses, and deviations from the plane-wave requirement of the incident light. Through careful choice of the materials and GMRF physical parameters, resonant reflection can be obtained for wavelengths ranging from the near ultraviolet[3] to the microwave regime, and has opened up vistas for a wide range of filtering,[4] biosensing,[5] and feedback[6] applications.

In this work, we have fabricated a GMRF that provides a spatially resolved resonant reflection for the externally incident optical beam based on its wavelength. The structure of the fabricated device is shown in Fig. 1. A low refractive index (RI) film is patterned with a periodic rectangular surface structure. Thereafter, a layer of high RI TiO_2 is deposited on the surface structure, such that the thickness of the film varies linearly along the direction perpendicular to the length of the surface structure. For such a design, the resonant wavelength is not constant across the device but also varies linearly along the gradient axis. Unlike previously fabricated structures,[7] this structure is not coupled to a separate waveguide. The existence of the layer 2 (Fig. 1) with the highest average index ensures that leaky modes can be excited within the periodically modulated layer itself. In the normal incidence regime of operation of this device, only the zeroth order waves exist outside the structure and are coupled to a symmetric resonance involving the ±1 evanescent diffracted orders. This symmetric coupling results in the second order Bragg condition being satisfied[8] and causes strong in-plane confinement of the resonant mode via a standing wave. The fabrication and resonance characteristics of this device have already been presented,[9] but for the sake of clarity are summarized as follows: Firstly, a silicon master is patterned by conventional lithographic and etching processes so as to posses a one-dimensionally periodic surface structure of period $\Lambda=550$ nm and step height $h=170$ nm. Thereafter, the structure is replicated in a soft elastomeric stamp prepared by curing polydimethylsiloxane (PDMS) on the silicon master. The PDMS stamp is then pressed onto a glass substrate onto which a low RI spin on glass (Nanoglass, Honeywell) is coated, followed by thermal curing, which results in replication of the original surface structure on the glass slide. Finally, a linearly graded layer of high RI TiO_2 is deposited on this structure, with thickness ranging from 160 to 245 nm, across a distance of 26 mm. In the reflection spectrum for this device illuminated with TM-polarized (electric field polarized perpendicular to the length of the surface structure) white light, a resonant reflection was seen to linearly range from $\lambda=798.0$ nm to $\lambda=909.0$ nm,

a)Electronic mail: bcunning@uiuc.edu

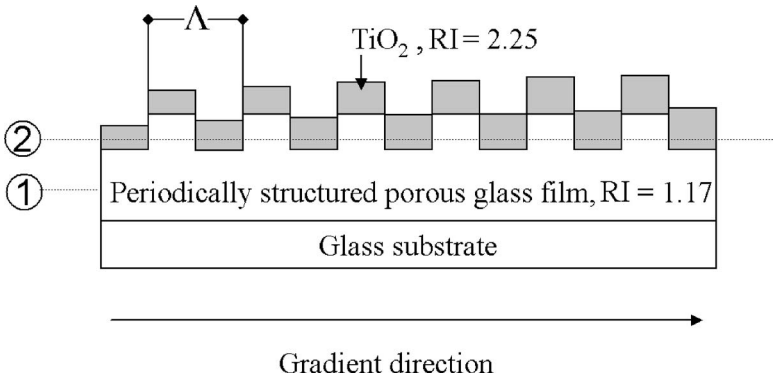

FIG. 1. Cross section schematic of the GWF structure as fabricated. Here, $\Lambda = 550$ nm denotes the period of the structure, and the numeric labels represent the (1) substrate film and (2) periodically modulated layer. The thickness of the TiO_2 layer is varied in the direction shown, such that an increase of 1 nm thickness occurs every 556 periods.

with a peak reflectivity of ~75% at $\lambda = 855.0$ nm. The bandwidth at $\lambda = 855.0$ nm (full width at half maximum) was ~10 nm.

The GWF (active area of 10×10 mm^2) was mounted on a CCD line camera (LC1-USB, Thorlabs). TM-polarized incident light from a tunable near-infrared laser (Velocity 6316, New Focus) was expanded to approximately match the active area. By expanding the beam and allowing it to be incident on the GWF, we ensure that only within the region of the GWF which is resonant with the incident wavelength, light will be reflected back, resulting in a transmission minimum being recorded by the CCD. As the wavelength is changed, the incident light will be resonant at a different region of the GWF and the position of the transmission minimum will change. The wavelength of the laser was tuned from $\lambda = 843.0$ nm to $\lambda = 853.0$ in steps of 1.0 nm at a constant power of 2.4 mW, and the resulting intensity spectrum was recorded on the CCD camera connected to a computer. Figure 2 shows the as-recorded spectrum for three wavelengths, i.e., $\lambda = 843.00$ nm, $\lambda = 848.00$ nm, and $\lambda = 853.00$ nm versus the pixel number along the CCD. The pixels are equally spaced at an interval of 7 μm. The effect of the GWF on the location of the transmission minimum is clearly seen in this spatially resolved intensity profile. As the wavelength of the incident beam is changed, the location of the transmission minimum varies spatially and this can be used to calibrate the pixel scale shown in Fig. 2. The spatial intensity profile, however, follows a broadened version of the Lorentzian profile of the resonance. This is explained by the fact that due to the relatively large bandwidth of the resonance, adjacent resonances that peak at different wavelengths have contributing components in the transmission dip. This can be easily overcome by designing the filter to have very narrow-band resonances and/or creating a stronger gradient in the deposition of the TiO_2.

The sensitivity of the setup was determined by plotting the wavelength of the incident laser beam versus the pixel number, for which an intensity minimum was recorded on the CCD camera. Due to the reason outlined above (broadened transmission dips) and random electronic noise in the CCD-computer interface, it was impossible to clearly define with single pixel resolution, a minimum in the transmitted spectrum. To overcome this, the intensity profile was processed by fitting to a Lorentzian function (inset, Fig. 3), and its peak corresponding to the peak wavelength value (PWV) of the source was determined. Such a fitting-regression process improves the resolution of detection for the system, as the minima can now be estimated within fractions of pixels, however, at the cost of inaccuracy introduced by the fitting process. Figure 3 shows the sensitivity of the system to

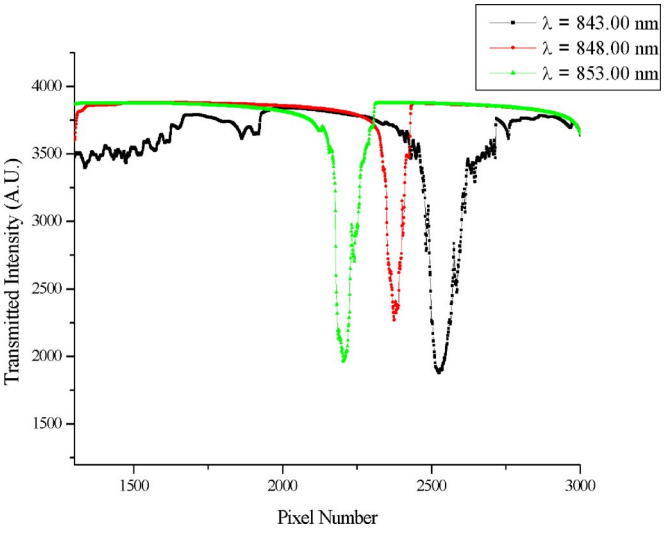

FIG. 2. (Color online) Intensity spectrum of the incident beam as recorded by the system for three wavelengths. Only regions that are resonant with the incoming beam present a dip in transmission. As the wavelength of the incident beam is changed, the resonance occurs at a different spatial location and presents a shifted transmission dip. The distance between adjacent pixels is 7 μm.

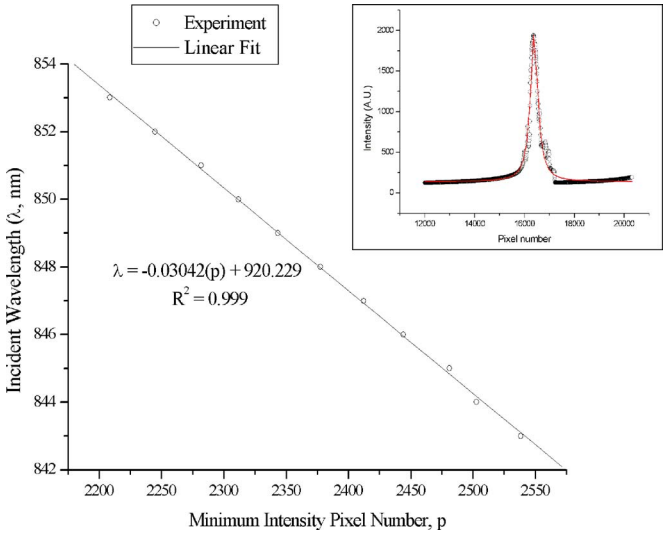

FIG. 3. (Color online) Position of the transmission minimum in pixel number (as determined by curve fitting) vs the incident wavelength. The solid line represents the line fit to the data and shows a high degree of linearity. The equation describes the line and the sensitivity characteristics of the system. (Inset): Lorentzian fit for the data point corresponding to $\lambda = 849.00$ nm.

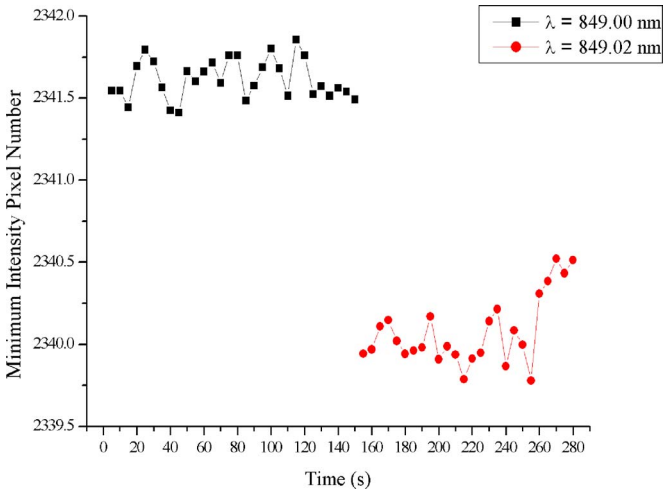

FIG. 4. (Color online) Time-resolved dispersion of the pixel for which minimum intensity was detected by the system for set wavelengths of $\lambda=849.00$ nm (boxes) and $\lambda=849.02$ nm (circles).

changes in wavelength of the incident beam. As expected, the location of the calculated intensity minimum (minimum intensity pixel number) moves linearly along the CCD as the wavelength is increased. The slope of this line gives us information regarding the sensitivity of the system and is calculated to be 0.0304 nm/pixel.

The resolution of the system was determined by first plotting the pixel number for which the intensity minimum was recorded versus time, for a fixed wavelength, $\lambda=849.00$ nm. For this measurement, intensity spectra were captured every 5 s, at an integration time of 30 μs for the CCD and taking 42 samples per average. This resulted in a time-resolved dispersion of the minimum intensity pixel number. From this dispersion, we determine that at a set wavelength of $\lambda=849.00$ nm, the standard deviation (σ) from the average minimum intensity pixel number was $\sim$0.12 pixels. Assuming a normal distribution, three times this value, i.e., 3σ ($\sim$0.36 pixels) will therefore be the minimum amount of shift required along the CCD to ensure accuracy of the next resolved wavelength within 99.73%. From the equation that describes the sensitivity of the system, we can deduce that $\Delta\lambda=0.0304(\Delta p)$ will be the resolution in nanometers, as described above. For $\Delta p=3\sigma=0.36$ pixels, we get a resolution $\Delta\lambda=0.011$ nm. The wavelength of the light emitted by the laser was increased from $\lambda=849.00$ nm to $\lambda=849.02$ nm (limited by the tuning resolution of the laser) and the time dispersion experiment was repeated. Figure 4 shows the time-resolved dispersion for the two wavelengths studied and is indicative of the fact that a change of 0.02 nm in wavelength can be resolved satisfactorily by the system. The PWV detected (as calculated from the equation inset in Fig. 3) by the system, however, does not exactly match the wavelength set for the laser. This is explained mainly due to the poor tuning repeatability of the laser (0.1 nm).

The wavelength detection system we have described and realized can be utilized for a wide variety of applications including identification of compounds via fluorescence spectroscopy, high-resolution laser wavelength detection, and rapid checking and testing of solid-state emitters such as light emitting diodes (LEDs) or organic LEDs. The advantages this system has to offer stem from the fact that it is compact and the GWF is fabricated very cost effectively by a replication process. Spatial and spectral resolutions can be significantly improved with narrow reflectance characteristic GWFs. In fact, by fabricating GWFs with subnanometer reflection linewidths, a low cost, portable spectrometer can be envisioned, wherein the spectrum of a broadband optical beam incident on the system would correspond to a broad transmission dip recorded by the CCD, the transmission dip being composed of individual, spatially, and spectrally resolved narrow bandwidth resonances. It is also possible to quadratically increase the dynamic range of the system by employing a two-dimensional lattice with a high index film graded in both directions of periodicity and a two-dimensional CCD array, which will be able to resolve individual wavelengths in a plane, in comparison to along a line, as we have shown.

In conclusion, we have demonstrated a compact, cost-effective system based on the guided-mode resonance effect to determine the peak wavelength value of an incident optical beam. The system is based only to two working components and can resolve wavelength changes down to 0.011 nm with over 99% accuracy.

This work was supported by the National Science Foundation under Grant No. 0427657. The experimental portion of this work was carried out in the Laser and Spectroscopy Facility of the Frederick Seitz Materials Research Laboratory, University of Illinois, which is partially supported by the U.S. Department of Energy under Grant No. DEFG02-91-ER45439. The authors thank Julio A. Soares for his facilitation of the use of the Laser and Spectroscopy Facility. Any opinions, findings, and conclusions or recommendations expressed in this material are those of the authors and do not necessarily reflect the views of the National Science Foundation.

[1] S. S. Wang and R. Magnusson, Appl. Opt. **32**, 2606 (1993).
[2] S. S. Wang, R. Magnusson, and J. S. Bagby, J. Opt. Soc. Am. A **7**, 1470 (1990).
[3] N. Ganesh, I. D. Block, and B. T. Cunningham, Appl. Phys. Lett. **89**, 023901 (2006).
[4] R. Magnusson and S. S. Wang, Appl. Phys. Lett. **61**, 1022 (1992).
[5] B. T. Cunningham, B. Lin, J. Qiu, P. Li, J. Pepper, and B. Hugh, Sens. Actuators B **81**, 316 (2002).
[6] T. Kobayashi, Y. Kanamori, and K. Hane, Appl. Phys. Lett. **87**, 151106 (2005).
[7] Z. S. Liu, S. Tibuleac, D. Shin, P. P. Young, and R. Magnusson, Opt. Lett. **23**, 1556 (1998).
[8] D. Rosenblatt, A. Sharon, and A. A. Friesem, IEEE J. Quantum Electron. **33**, 2038 (1997).
[9] D. W. Dobbs, I. Gershkovich, and B. T. Cunningham, Appl. Phys. Lett. **89**, 123113 (2006).